

Minimizing finite-size effects in artificial resonance tunneling structures

Philip Chak and J. E. Sipe

Department of Physics and Institute for Optical Sciences, University of Toronto, Toronto M5S 1A7, Canada

Received February 3, 2006; accepted May 9, 2006;

posted June 22, 2006 (Doc. ID 67757); published August 9, 2006

We consider finite-size effects in coupled cavity structures. Starting with microring resonator structures well described by transfer matrices, we obtain conditions that lead to the minimization of finite-size effects. Our approach does not require numerical optimization and requires only slight modification of design parameters guided by closed-form analytical expressions. Using a Breit–Wigner scattering formalism, we demonstrate that the scheme can be used to minimize finite-size effects in a general class of coupled cavity structures. The strength of the present technique lies in its simplicity and its applicability to a wide variety of structures described by tight-binding formalisms. © 2006 Optical Society of America
OCIS codes: 130.3120, 230.1150.

In recent years much attention has been paid to photonic coupled cavity (or resonant tunneling) structures,¹ in part because of their possible use in slow light applications. These structures can be well described by a tight-binding formalism, with each cavity weakly coupled to its nearest neighbors and with next-nearest neighbor interactions negligible. While the properties of these structures have been largely understood through dispersion relations,¹ which implicitly assume an infinite, periodic system, it is well known that in a realistic structure finite-size effects lead to Fabry–Perot fringes in the transmission spectrum.^{2,3} The various methods^{2–4} proposed to correct for finite-size effects have generally been based on numerical minimization schemes. However, an efficient analytical scheme based on an intuitive physical picture is still lacking.

In this paper we present a scheme that minimizes finite-size effects at and around a reference frequency, ω_{ref} . The basic idea is to slightly modify the physical parameters of the resonators at either end of the device such that the reflections cancel out the Fabry–Perot resonances at ω_{ref} , in effect providing an antireflection (AR) coating. Compared with previously proposed schemes, our scheme has the advantage that it carries a clear physical interpretation and does not require the use of numerical techniques. Our analysis, which is based on the standard transfer-matrix method (TMM) for optical structures,⁵ results in closed-form analytical expressions that determine the physical parameters of these end resonators.

It is well known that the transmission properties of 1D and quasi-1D structures can be described by 2×2 transfer matrices.^{5,6} For 1D lossless structures possessing mirror symmetry in the x direction and for quasi-1D structures possessing mirror symmetry in both the x and the y directions^{5,6} (see Fig. 1) the transfer matrix can be written as

$$\mathbf{M}(\omega) = \frac{1}{\tau(\omega)} \begin{bmatrix} e^{i\phi(\omega)} & \sqrt{1 - \tau^2(\omega)} e^{i\mu} \\ \sqrt{1 - \tau^2(\omega)} e^{-i\mu} & e^{-i\phi(\omega)} \end{bmatrix}, \quad (1)$$

where $\mu = \pm \pi/2$. In general, $t = \mathbf{M}_{22}^{-1} = \tau e^{i\phi}$ and $r = \mathbf{M}_{12}(\mathbf{M}_{22})^{-1} = \sqrt{1 - \tau^2} e^{i(\phi + \mu)}$ represent the transmis-

sion and reflection coefficients, respectively, and $\tau(\omega) = |t(\omega)|$ represents the transmission amplitude. For later convenience we define $\bar{\phi} = \phi - \rho\pi$ and $\bar{\mu} = \mu - \rho\pi$, with $\rho = (0, 1)$ as $(0 \leq \phi \leq \pi, \pi < \phi < 2\pi)$ such that $0 \leq \bar{\phi} \leq \pi$. With the new definition, the transfer matrix can be written as $\mathbf{M} = (-1)^\rho \bar{\mathbf{M}}$. Since \mathbf{M} and $\bar{\mathbf{M}}$ are unimodular, we can write the eigenvalues of $\bar{\mathbf{M}}$ as $e^{\pm i\zeta(\omega)}$ (with $0 \leq \zeta \leq \pi$). It is straightforward to show that

$$\cos \bar{\zeta}(\omega) = \frac{\cos \bar{\phi}(\omega)}{\tau(\omega)}. \quad (2)$$

The eigenvectors \mathbf{f}_\pm of $\bar{\mathbf{M}}$ can be written as $\mathbf{f}_\pm^T = [1 \ R_\pm]$ and $\mathbf{f}_\pm = [R_\pm^* \ 1]$, where

$$R_\pm(\omega) = \frac{-i\sqrt{1 - \tau^2} e^{-i\bar{\mu}}}{\tau \sin \bar{\zeta} + \sqrt{1 - \tau^2} \cos^2 \bar{\zeta}}. \quad (3)$$

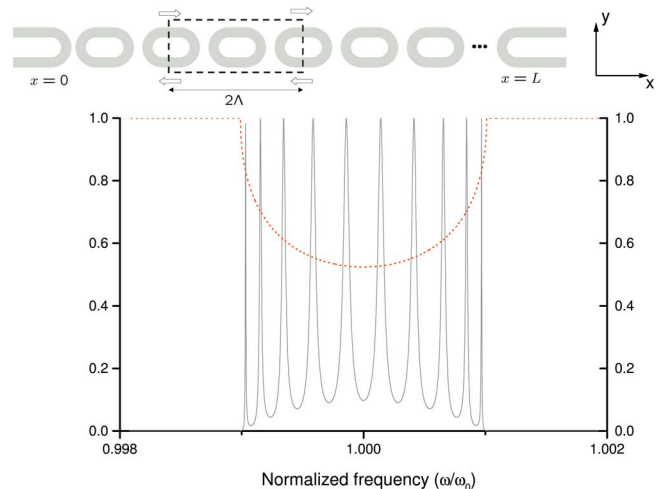


Fig. 1. (Color online) Top, schematic of a coupled microring resonator structure. The unit cell of the structure is enclosed within the dashed rectangle. Bottom, plot of $|t_N(\omega)|^2$ for $N=10$ (solid curve), $R_\infty(\omega)$ (dotted curve). All rings have effective index $n=3.0$, effective circumference $L=52.0 \mu\text{m}$, and cross-coupling coefficient $\sigma=0.95$.

We choose to work with $\bar{\phi}$ (and hence $\bar{\mathbf{M}}$) to avoid ambiguities of signs when constructing $R_\infty(\omega)$. Note that \mathbf{M} and $\bar{\mathbf{M}}$ share the same set of eigenvectors \mathbf{f}_\pm . The quantity $R_\infty(\omega)$ can be interpreted as the reflectivity of the corresponding semi-infinite structure.⁷ Last, it is apparent from Eq. (3) that for frequencies where $\bar{\zeta}(\omega)$ is real, $R_\infty(\omega)$ is completely real and can take on the values $\angle R_\infty(\omega) = 0$ or π .

We now consider the structure depicted in Fig. 1 (top), which consists of directly coupled microring resonators.^{8,9} We identify a resonance frequency ω_0 satisfying $\omega_0 nL/c = 2\pi l$ (with $l \in I$ indexing the resonance order), and let n and L denote the effective index and effective circumference of the resonators forming the structure. In what follows we restrict ourselves to frequencies in close vicinity of ω_0 and further identify the resonance as an odd (even) resonance if l is an odd (even) integer. Using the TMM, the transmission through each unit cell of the structure can be written as $\mathbf{M}(\omega) = \mathbf{P}(\omega)\boldsymbol{\Sigma}\mathbf{P}(\omega) \cdot \mathbf{P}(\omega)\boldsymbol{\Sigma}\mathbf{P}(\omega)$, where \mathbf{P} represents the phase accumulation on propagation through a quarter of the ring and $\boldsymbol{\Sigma}$ is the coupling matrix describing the coupling of electric fields between adjacent rings. This explicit form for $\mathbf{M}(\omega)$ corresponds to the approximation that the coupling of electric fields occurs only at the point of smallest separation between two adjacent rings. The matrices $\mathbf{P}(\omega)$ and $\boldsymbol{\Sigma}$ can be written explicitly as

$$\mathbf{P}(\omega) = \begin{bmatrix} e^{i\omega nL/4c} & 0 \\ 0 & e^{-i\omega nL/4c} \end{bmatrix}, \quad \boldsymbol{\Sigma} = (i\kappa)^{-1} \begin{bmatrix} -1 & \sigma \\ -\sigma & 1 \end{bmatrix}. \quad (4)$$

The self- and cross-coupling coefficients σ and κ in $\boldsymbol{\Sigma}$ are real, frequency-independent quantities satisfying $\sigma^2 + \kappa^2 = 1$,⁸ as required by conservation of energy. In light of Eqs. (4), we define $\mathbf{T} = \mathbf{M}^{1/2} = \mathbf{P}(\omega)\boldsymbol{\Sigma}\mathbf{P}(\omega)$ and obtain an explicit expression for $R_\infty(\omega)$ by relating eigenvectors of \mathbf{T} to eigenvectors of $\bar{\mathbf{M}}$. This results in

$$R_\infty(\omega) = (-1)^l \sigma (\kappa \sin \psi + \sqrt{1 - \kappa^2 \cos^2 \psi})^{-1}, \quad (5)$$

with

$$\psi(\omega) = \arccos[(\omega - \omega_0)/\Gamma], \quad \Gamma \equiv 2\kappa c/nL. \quad (6)$$

The transmission of a finite structure consisting of N cavities [and hence $(N+1)/2$ unit cells] can be calculated as $|t_N(\omega)|^2 = |\mathbf{M}_{22}(\omega)Y_{N-1}(\omega) - Y_{N-2}(\omega)|^{-2}$, where $Y_N(\omega) = [\sin \bar{\zeta}(\omega)] \sin[(N+3)\bar{\zeta}(\omega)/2]$.⁵ A typical transmission spectrum, for a finite structure consisting of $N=10$ cavities, is shown in Fig. 1 (bottom). It is apparent that the transmission spectrum exhibits Fabry–Perot fringes, with high transmission attained only at certain frequencies. To suppress these fringes, we introduce an AR structure at the two ends. The purpose of the AR structure is to cancel out reflections induced by the finite structure at some chosen frequency ω_{ref} . With \mathbf{M}' denoting the transfer matrix of the AR structures at both ends, complete cancellation of reflection at ω_{ref} can be achieved if $R_\infty(\omega_{\text{ref}})$ is related to the matrix elements of \mathbf{M}' by

$R_\infty(\omega_{\text{ref}}) = r_{\text{AR}}^*(\omega_{\text{ref}}) = \mathbf{M}'_{21}(\mathbf{M}'_{11})^{-1}$, where r_{AR} denotes the reflection induced by the AR element. We arrived at this condition by considering the transmission across the AR structure; note that in a reversible structure the AR element that minimizes reflection at the first interface ($x=0$) is identical to the AR element that minimizes reflection at the second interface ($x=L$), owing to the time-reversal properties of Maxwell's equations. We design the AR structure such that it resembles the unit cell depicted in Fig. 1 (top), albeit with a different circumference and nearest-neighbor coupling strength. For the microring structures we consider two different AR implementations. We first consider the case in which the transfer matrix for the AR structure can be written as $\mathbf{M}'(\omega) = \mathbf{P}(\omega)\boldsymbol{\Sigma}\mathbf{P}(\omega) \cdot \mathbf{P}'(\omega)\boldsymbol{\Sigma}'\mathbf{P}'(\omega)$. Here

$$\mathbf{P}'(\omega) = \begin{bmatrix} e^{i\theta'(\omega)} & 0 \\ 0 & e^{-i\theta'(\omega)} \end{bmatrix}, \quad \boldsymbol{\Sigma}' = (i\kappa')^{-1} \begin{bmatrix} -1 & \sigma' \\ -\sigma' & 1 \end{bmatrix}, \quad (7)$$

represent the new phase accumulation and unimodular coupling coefficients at the first and last unit cells, as required to form an AR structure. Analogous to Eqs. (4), we have $\theta' = \omega nL'/4c$, where $(L+L')/2$ represents the circumference of the AR ring. Using the explicit expressions for $\mathbf{P}'(\omega)$ and $\boldsymbol{\Sigma}'$, and noting that \mathbf{f}_+ also serves as eigenvector of $\mathbf{T} = \mathbf{P}(\omega)\boldsymbol{\Sigma}\mathbf{P}(\omega)$, one can show $R_\infty = \mathbf{M}'_{21}(\mathbf{M}'_{11})^{-1}$ is satisfied when $\sigma' \exp[-2i\theta'(\omega_{\text{ref}})] = R_\infty(\omega_{\text{ref}})$, leading to

$$2\theta'(\omega_{\text{ref}}) = \begin{cases} \pi & \text{odd } l \\ 0 & \text{even } l \end{cases}, \quad (8)$$

$$\sigma' = |R_\infty| = \sqrt{\eta^2 + 1} - \eta, \quad (8)$$

with

$$\eta(\omega_{\text{ref}}) = \sigma^{-1} \sqrt{1 - \sigma^2} \sin \psi(\omega_{\text{ref}}). \quad (9)$$

Alternatively, the AR structure can be designed such that it differs from a normal unit cell only by its nearest-neighbor coupling (in other words, the circumference of the AR structure is the same as a normal unit cell). In this case the transfer matrix can be written as $\mathbf{M}'(\omega) = \mathbf{P}(\omega)\boldsymbol{\Sigma}''\mathbf{P}(\omega) \cdot \mathbf{P}(\omega)\boldsymbol{\Sigma}'\mathbf{P}(\omega)$, with

$$\boldsymbol{\Sigma}'' = (i\kappa'')^{-1} \begin{bmatrix} -1 & \sigma'' \\ -\sigma'' & 1 \end{bmatrix}.$$

Cancellation of reflection at ω_{ref} can be achieved with

$$\sigma'' = \sigma(1 + \kappa^2)^{-1/2}, \quad \sigma' = \sqrt{4\eta^2 + 1} - 2\eta, \quad (10)$$

keeping η as defined in Eq. (9). One can verify that the two AR structures [designed according to Eqs. (8) or (10)] lead to essentially the same transmission spectrum within the approximation $\sigma \approx 1$. The effectiveness of the AR structure is demonstrated in Fig. 2. We show the transmission spectrum of the finite structure with and without the AR structure at both ends, using $\omega_{\text{ref}} = \omega_0$. It is apparent that although the AR coating is designed to achieve perfect transmis-

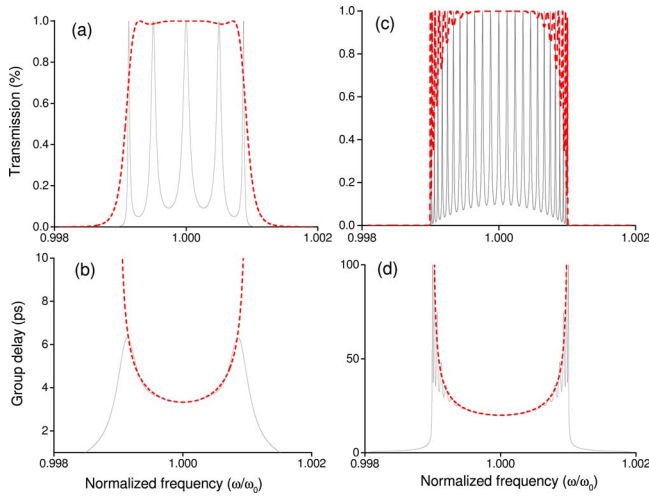


Fig. 2. (Color online) Transmission and group delay for finite structures with (a), (b) 5 and (c), (d) 25 cavities, using parameters listed in Fig. 1. (a), (c) Comparison of transmission for structures with (dashed) or without (solid) AR modification. (b), (d) Comparison of delay for a structure with AR (dashed) and corresponding delay within an infinite structure (solid).

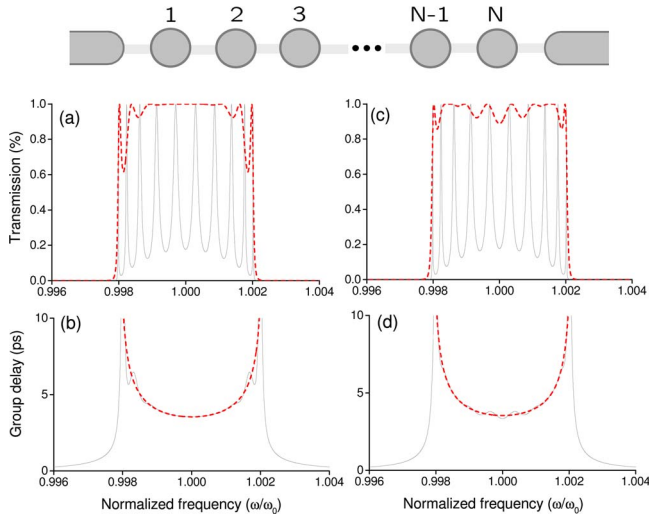


Fig. 3. (Color online) (top) Schematic of the finite coupled cavity structure discussed in the text. We used $\delta_0 = 4.2 \times 10^{-3}$, with AR elements constructed by using Eqs. (11). (a), (c) Comparison of transmission for structures with (dotted) or without (solid) AR modification. (b), (d) Comparison of delay for a structure with AR (dashed) and corresponding delay within an infinite structure (solid). In (a) and (b) $\psi = \pi/2$ such that $\omega_{\text{ref}} = \omega_0$; in (c) and (d) $\psi = \pi/4$ such that $\omega_{\text{ref}} = \omega_0 \pm \sqrt{2}\Gamma$.

sion only at ω_{ref} , in practice the transmission is improved over an appreciable range of frequencies. This is attributed to the fact that in the weak coupling regime (which is typically the regime of interest) the passband is narrow in frequency. In the more general case a thorough numerical optimization of the coupling coefficients² can be used.

Using results derived from TMM, we now generalize the result to general coupled cavity structures

well described by the generalized Breit–Wigner formalism (e.g., photonic crystal coupled cavity structures). The schematic of a typical structure is depicted in Fig. 3. It consists of single-mode cavities end coupled to two single-mode channels. Following Sumetsky and Eggleton,² the transmission coefficient can be written as $t_N(\omega) = \gamma \mathbf{U}_{1,N}$, where \mathbf{U}_{ij} represents matrix elements of $\mathbf{U}(\omega) \equiv \mathbf{\Lambda}^{-1}(\omega)$. The matrix $\mathbf{\Lambda}(\omega)$ is defined as²

$$\mathbf{\Lambda}(\omega) = \begin{bmatrix} \omega - \omega_0 + \frac{i\gamma}{2} & \delta_{12} & 0 & \dots & 0 \\ \delta_{21} & \omega - \omega_0 & \delta_{23} & \dots & 0 \\ \dots & \dots & \dots & \dots & \dots \\ 0 & 0 & 0 & \dots & \omega - \omega_0 + \frac{i\gamma}{2} \end{bmatrix},$$

where $\gamma/2$ represents the decay rate of the first (last) cavity due to the cavity–channel coupling and δ_{ij} represents nearest-neighbor coupling strength. The parameters for the AR structure discussed above [Eqs. (10)] correspond to a modification of the coupling coefficients and decay rates such that

$$\gamma/2 = 2\delta_0 \sin \psi(\omega_{\text{ref}}), \quad \delta_{1,2} = \delta_{N,N-1} = \sqrt{2}\delta_0, \quad (11)$$

and all other coupling coefficients are denoted δ_0 . We demonstrate the effectiveness of our scheme in Fig. 3, where the transmission amplitude and group delay of a finite structure with ten cavities are shown. It is apparent that, by extending the AR scheme presented for the microring cavity case, closed-form analytical expressions for the coupling coefficients and decay rates are obtained.

This work was supported by Photonics Research Ontario and the DARPA. P. Chak (pchak@physics.utoronto.ca) acknowledges receiving an Ontario Graduate scholarship and helpful discussion with Suresh Pereira.

References

1. A. Yariv, Y. Xu, R. K. Lee, and A. Scherer, *Opt. Lett.* **24**, 711 (1999).
2. M. Sumetsky and B. J. Eggleton, *Opt. Express* **11**, 381 (2003).
3. P. Sanchis, J. García, A. Martínez, and J. Martí, *J. Appl. Phys.* **97**, 013101 (2005).
4. M. Sumetsky, *J. Phys. Condens. Matter* **3**, 2651 (1991).
5. A. Yariv and P. Yeh, *Optical Waves in Crystals* (Wiley, 1983).
6. P. Chak and J. E. Sipe, “Time reversal of light propagation in periodic quasi-1D structures by symmetry transformation,” manuscript in preparation.
7. G. Boedeker and C. Henkel, *Opt. Express* **11**, 1590 (2003).
8. J. E. Heebner, P. Chak, S. Pereira, J. E. Sipe, and R. W. Boyd, *J. Opt. Soc. Am. B* **21**, 1818 (2004).
9. J. Poon, J. Scheuer, S. Mookherjea, G. T. Paloczi, Y. Huang, and A. Yariv, *Opt. Express* **12**, 90 (2004).